In Vivo Assessment of Drug Efficacy against Mycobacterium abscessus Using the Embryonic Zebrafish Test System

Audrey Bernut, Vincent Le Moigne, Tiffany Lesne, Georges Lutfalla, Jean-Louis Herrmann, Laurent Kremer

HAL Id: hal-02088311

https://hal.umontpellier.fr/hal-02088311

Submitted on 11 Apr 2019

1   ***In vivo* assessment of drug efficacy against *Mycobacterium***

2   ***abscessus* using the embryonic zebrafish test system**

3

4   **Audrey Bernut[1], Vincent Le Moigne[3], Tiffany Lesne[1], Georges Lutfalla[1],**

5   **Jean-Louis Herrmann[3] and Laurent Kremer[1,2,#]**

6

7

8   [1]Laboratoire de Dynamique des Interactions Membranaires Normales et Pathologiques, CNRS

9   UMR5235, Université Montpellier 2, Montpellier, France ;

10   [2]Inserm, DIMNP, Place Eugène Bataillon, 34095 Montpellier Cedex 05, France.

11   [3]EA3647-EPIM, UFR des Sciences de La Santé; Université de Versailles St Quentin, 2 avenue de

12   la Source de la Bièvre, 78180 Montigny le Bretonneux, France.

13

14

15   [#]To whom correspondence should be addressed:

16   Tel: (+33) 4 67 14 33 81, Fax: (+33) 4 67 14 42 86, E-mail: laurent.kremer@univ-montp2.fr

17

18   **Keywords:** *M. abscessus*, zebrafish, drug testing, optical imaging, infection

19

20   **Running title:** *In vivo* imaging for anti-*M. abscessus* drug testing

21

22

ABSTRACT

Mycobacterium abscessus is responsible of a wide spectrum of clinical syndromes and is one of the most intrinsically drug-resistant mycobacterial species. Recent evaluation of the *in vivo* therapeutic efficacy of the few potentially active antibiotics against *M. abscessus* was essentially performed using immune-compromised mice. Herein, we assessed the feasibility and sensitivity of fluorescence imaging for monitoring the *in vivo* activity of drugs against acute *M. abscessus* infection using zebrafish embryos. A protocol was developed where clarithromycin and imipenem were directly added to water containing fluorescent *M. abscessus*-infected embryos in a 96-well plate format. The status of the infection with increasing drug concentrations was visualized on a spatiotemporal level. Drug efficacy was assessed quantitatively by determining the index of protection, the bacterial burden by CFU plating and by monitoring the number of abscesses through fluorescence measurements. Both drugs were active in infected embryos and were capable of significantly increasing embryo survival in a dose-dependent manner. Protection from bacterial killing correlated with restricted mycobacterial growth in the drug-treated larvae and with reduced pathophysiological symptoms, such as the number of abscesses within the brain. In conclusion, we present here a new and efficient method for testing and compare the *in vivo* activity of two clinically-relevant drugs based on a fluorescent reporter strain in zebrafish embryos. This approach could be applied to a rapid determination of *in vivo* drug susceptibility profile of clinical isolates and to assess the preclinical efficacy of new compounds against *M. abscessus*.

INTRODUCTION

M. abscessus (*Mabs*) is an emerging pathogen and the etiological agent of a wide spectrum of infections in humans. It is responsible for severe chronic pulmonary and disseminated infections, mostly in immunosuppressed and in cystic fibrosis (CF) patients (1), and cutaneous diseases, often post-traumatic and post-surgical. This neglected pathogen causes a higher fatality rate compared to other RGMs and the infection of CF patients is becoming a major health-related issue in most CF centers worldwide (2). *Mabs* infections occur in early childhood (3), are severe and sometimes fatal, especially following transplantation (4-6), and have the potential to cause outbreaks of infection (6). *Mabs* is also the main RGM responsible for nosocomial and iatrogenic infections in humans (post-injection abscesses, cardiac surgery, and plastic surgery) (7-9). It has also been reported to cross the blood-brain barrier and to cause important central nervous system (CNS) lesions. Although a rapid grower, *Mabs* possesses several important pathogenic traits such as the ability to i) persist silently for years and even decades (10) in the human host, and to ii) induce lung disease associated with caseous lesions and granuloma formation in lung parenchyma (11, 12).

The major issue with *Mabs* relies on its intrinsic resistance to the majority of available antibiotics. The American Thoracic Society has recommended different groups of agents, namely macrolides (clarithromycin), aminoglycosides (amikacin), cephamycins (cefoxitin) and carbapenems (imipenem) for treatment of *Mabs* infections (13). Patients with severe infections are generally treated with long courses of combinatorial antibiotic therapy, often accompanied by surgical resection. As antibiotic susceptibility testing is not fully standardized, the clinical response to drugs does not correlate well with *in vitro* susceptibility test results and failure occurs frequently despite administration of two or three antibiotics for several months (14).

69   This further emphasizes the need of suitable animal models (15, 16). In addition, different

70   clinical isolates of this emerging pathogen are not uniformly susceptible to the currently used

71   antibiotics (17). As a consequence, an optimal regimen to cure the *Mabs* infections has not

72   been yet established.

73   Thanks to the recent availability of efficient genetic tools (18), *Mabs* has been proposed as

74   an attractive experimental model to study non-tuberculous mycobacteria associated diseases

75   (1). Our poor understanding of the pathogenesis of *Mabs,* essentially hampered by the

76   restricted panel of cellular/animal models available, prompted us to develop the zebrafish

77   model of infection to describe the chronology of *Mabs* infection (19). In particular, the

78   *Mabs*/zebrafish couple already provided important insights regarding the pathogenesis of *Mabs*

79   such as the unexpected tropism for the CNS, a finding relevant in the light of recent clinical

80   studies reporting the presence of *Mabs* in the CNS of infected human patients (20, 21). Since

81   infection foci/abscesses within the CNS, particularly the brain, appear very rapidly and are very

82   easy to detect and visualize, we reasoned that this alternative model could represent a valuable

83   and cheap system to evaluate and compare the *in vitro* and *in vivo* activity of drugs against

84   *Mabs*. Such a simple and innovative system would be particularly suited for screening active

85   molecules and/or antibacterial activity assessment, representing a critical step in the context of

86   drug discovery, urgent in the case of *Mabs*.

87   Here, we report on the development of experimental conditions for *in vivo* imaging of

88   *Mabs* and demonstrate that it is compatible with *in vivo* observations, at a spatiotemporal

89   level, of the effects of drug treatment on the infection process. This represents a unique

90   biological model that allows non-invasive observations to evaluate, in real time, the efficacy of

91   antibiotics in living infected vertebrates, a system that could be applied to high-throughput *in*

92   *vivo* testing of drug efficacy against the most drug-resistant mycobacterial species.

93

MATERIALS AND METHODS

M. abscessus strains and growth conditions

The rough variant of *M. abscessus sensu stricto* strain CIP104536[T] (ATCC19977T) was grown at 30°C in Middlebrook 7H9 broth supplemented with 10% Oleic acid/Albumin/Dextrose/Catalase (OADC) enrichment and 0.05% Tween 80 (7H9[T]) or on Middlebrook 7H10 agar containing 10% OADC. Recombinant *Mabs* carrying pTEC27 (Addgene, plasmid 30182) that allows to express tdTomato under the control of a strong mycobacterial promoter were grown in the presence of hygromycin 500 mg/L (19).

Mice experiments and CFU counting

6-8 weeks old BALB/c mice were divided in groups of 5-7 mice and used for either intravenous (*i.v.*) or aerosol challenges. Inocula were prepared from rapidly thawed frozen aliquots, and bacterial clumps were eliminated by iterative passages through a 29.5-gauge insulin needle (Becton Dickinson). Bacterial suspensions were then diluted in phosphate buffer saline (PBS). For *i.v.* inoculations, 10^6 CFU (in 200 µl) were injected into the lateral tail/caudal vein, as previously described (22, 23). Pulmonary infections were achieved with aerosolized *Mabs* using an aerosol generator, equipped with a Micro Mist® small volume nebulizer (Hudson RCI-Teleflex medical) containing 6 ml of bacterial solution at 4×10^7 CFU/ml. Pre-sleeping mice (isoflurane® Abbott) were anesthetized with 200 µl of Hypnomidate (Etomidate®, Janssen-Cilag) and placed into an opened 50 ml syringe fixed on the top of a closed compartment containing the nebulizer. In this device, nebulization lasted for 15 min to vaporize the entire bacterial suspension. Lungs, liver and spleen were collected in PBS, crushed and 10-fols serial dilutions were plated on Middlebrook 7H11 plates for CFU counting, as previously described (22, 23).

118 Plates were then incubated at 37°C for up to 7 days. The results were expressed as the mean

119 Log_{10} CFU per organ.

120

121 **Minimal inhibitory concentrations**

122 Antibiotics powder tested in drug susceptibility assays were pharmaceutical standards for

123 imipenem/cilastatin (Mylan) or clarithromycin (Sigma-Aldrich). Stock solutions were dissolved

124 in water (imipenem) or in DMSO (clarithromycin). Drug susceptibility testing was also

125 determined using the microdilution method, in cation-adjusted Mueller-Hinton broth,

126 according to the Clinical and Laboratory Standards Institute (CLSI) guidelines (24). In addition,

127 the susceptibility profile was also determined on LB agar supplemented with increasing

128 concentrations of the compounds. Serial 10-fold dilutions of each actively growing culture were

129 plated and incubated at 37°C for 3-4 days and the MIC was defined as the minimum

130 concentration required to inhibiting 99% of the growth.

131

132 **Zebrafish care**

133 All zebrafish experiments were done at the University Montpellier 2, according to

134 European Union guidelines for handling of laboratory animals

135 (http://ec.europa.eu/environment/chemicals/lab_animals/home_en.htm) and approved by the

136 Direction Sanitaire et Vétérinaire de l'Hérault and Comité d'Ethique pour l'Expérimentation

137 Animale de la région Languedoc Roussillon (CEEA-LR) under the reference CEEA-LR-13007.

138 Experiments were performed using the *golden* ZF mutant (25). Eggs were obtained by natural

139 spawning and incubated at 28.5°C in water with 60 mg/L Ocean salts. Ages of the embryos are

140 expressed as hours post fertilization (hpf).

141

142   **Microinjection of *M. abscessus* into embryos**

143   Mid-log phase cultures of *Mabs* expressing tdTomato were centrifuged, washed and

144   resuspended in PBS supplemented with 0.05% Tween-80 (PBS^T). Bacterial suspensions were

145   then homogenized through a 26-gauge needle and sonicated three times for 10s and the

146   remaining clumps were allowed to settle down to for 5-10 min. Bacteria were concentrated to

147   an OD_{600} of 1 in PBS^T and *i.v.* injected (≈2nL containing 300 CFU) into the caudal vein in 30hpf

148   embryos previously dechorionated and anesthetized. To follow infection kinetics and embryo

149   survival, infected larvae were transferred into 96 well plates (2 embryos/plate) and incubated

150   at 28.5°C. The inoculum size was checked by injection of 2nL in sterile PBS^T and plated on

151   Middlebrook 7H10 agar containing 10% OADC supplemented with hygromycin 500 mg/L.

152

153   **Drug efficacy assessment in *Mabs*-infected ZF**

154   Clarythromycin and imipenem**/**cilastatin were added at one day post-infection (dpi),

155   directly into the water containing the embryos. Three doses were tested, corresponding to

156   1.7X, 17X and 170X the MIC of clarithromycin and 0.5X, 5X or 28X the MIC of imipenem, based

157   on the values determined using the microdilution method (Table S1). *In vivo* drug efficacy was

158   determined for each concentration by following i) the bacterial burdens, ii) the kinetic of

159   embryo survival, iii) the evolution of the infection foci/abscesses within the CNS and iv) the

160   effect on bacterial cord formation/reduction. Survival curves were determined by recording

161   dead embryos (no heartbeat) every day for up to 13 days. Regarding the kinetic of

162   mycobacterial loads, groups of three infected embryos were collected, lysed individually in 2%

163   Triton X100- PBS^T with a 26-gauge needle (15 up-and-down sequences) and resuspended in

164   PBS^T. Several 10-fold dilutions of homogenates were plated on Middlebrook 7H10 agar

165   supplemented with 10% OADC, the appropriate antibiotics and added of mix of "BBL™ MGIT™

7

166 PANTA^{TM}" (Becton-Dickinson) using as recommended by the supplier. CFU were enumerated

167 after 4 days of incubation at 30°C. This procedure was repeated at 0, 3, 5 dpi.

168

169 **Microscopy**

170 Widefield bright-field and fluorescence live microscopy of infected embryos were

171 performed using an Olympus MVX10 epifluorescent microscope equipped with a X-Cite$^{®}$120Q

172 (Lumen Dynamics) 120W mercury light source. Images are acquired with a digital color camera

173 (Olympus XC50) and processed using CellSens software (Olympus). Fluorescence filter cube

174 TRITC-MVX10 is used for detection of red light. For live imaging, anesthetized infected embryos

175 were positioned in dishes and immobilized with 1% low-melting point agarose solution covering

176 the entire larvae then immobilized embryos are immersed with fish water containing tricaine

177 for direct visualization.

178

179 **Image Processing and Analysis**

180 Final images analysis and visualization are performed using GIMP 2.6 freeware to merge

181 fluorescent and DIC images and to adjust levels and brightness and to remove out-of-focus

182 background fluorescence.

183

184 **Statistical Analyses**

185 Statistical analyses of comparisons between Kaplan-Meier survival curves were performed

186 using the log rank test with Prism 4.0 (Graphpad, Inc). CFU counts and quantifications

187 experiments were analyzed using one-way ANOVA and Fisher's exact test, respectively.

188 Statistical significance was assumed at p values <0.05.

189

RESULTS

191 ***M. abscessus* fails to establish a persistent infection in BALB/c mice**

192   Experiments were first aimed to determine the colonization rate of *Mabs* in a murine

193 pulmonary infection model (Figure 1A). Aerosol infections of BALB/c mice was characterized by

194 an initial and rapid increase of the bacterial burden from 1-3 days post-infection (dpi) in the

195 lungs, followed by a phase of infection control that leads to a reduction (starting after 3dpi) and

196 almost complete clearance of the bacilli at 27dpi. Very few bacteria were detected within the

197 spleen or the liver of infected mice. The colonization profile after an *i.v.* challenge showed that

198 bacilli were primarily found in the liver at 1dpi and to a lesser extent in the spleen and the lungs

199 (Figure 1B). All heavily infected organs rapidly underwent a progressive reduction in the CFU

200 levels with a 3-Log_{10} CFU decrease in the liver and the lungs at 30dpi, highlighting a transient

201 colonization process. These results indicate that the course of infection in immune-competent

202 mice consists mostly as a progressive eradication of the pathogen. This model would, therefore,

203 require to testing a very large number of animals to insure that the observed CFU decrease

204 results to the antibiotic regimen rather than to the natural course of infection. Consequently,

205 wild-type BALB/c mice are not well adapted to investigate the *in vivo* efficacy of therapeutic

206 treatments.Therefore, the use of alternative animal models susceptible to *Mabs* infection,

207 permissive to bacterial replication and leading to the development of infection foci/abscesses

208 and death would be particularly advantageous. We hypothesized that ZF larvae may represent a

209 valuable system for *in vivo* assessments of drugs against *Mabs*.

210

211   **Zebrafish larvae for *in vivo* assessment of drug activity in *M. abscessus***

212   To assess *in vivo* antimycobacterial drug activity against *Mabs* in ZF larvae, an experimental

213 protocol has been established (Figure 2). tdTomato-expressing *Mabs,* exhibiting red

214   fluorescence, were *i.v.* injected in the caudal vein of embryos at 30 hours post-fertilization (hpf)

215   and transferred into 96-well plates. Antibiotic were then directly added at 1dpi to the water

216   containing the infected embryos and the drug-supplemented water was then changed on a

217   daily basis for 5 days. Daily monitoring of mortality as well as determination of the bacterial

218   burden at various time points were used as phenotypic read-outs. Thanks to the optical

219   transparency of the embryos, the effect of the antibiotic treatment on evolution of the clinical

220   signs of infection was also recorded by fluorescence microscopy. Since most infected *Mabs*

221   infected-embryos developed infection abscesses within the CNS, especially the brain (Figure 2),

222   the chemotherapeutic activity of the antibiotics was particularly easy to observe, on an

223   individual basis, during the entire period of drug treatment. Drug-mediated toxicity was also

224   investigated by determining the survival curves of non-infected embryos treated with

225   increasing drug doses. We have previously shown that the rough *Mabs* exhibits a marked

226   neurotropism with massive abscesses within the CNS (19), thus prompting us to assess the

227   activity of drugs in *Mabs*-infected embryos with a special emphasis on infection within the CNS.

228

229   **Minimal inhibitory concentrations of antimycobacterial drugs against *M. abscessus***

230   We first determined the *in vitro* activity of various drugs, including antitubercular agents,

231   against *Mabs* using the microdilution in cation-adjusted Mueller-Hinton broth, according to the

232   Clinical and Laboratory Standards Institute guidelines (24). Table S1 shows that the activity

233   varies considerably, in agreement with other studies. The first-line antitubercular drug isoniazid

234   and second-line drug thiacetazone appeared inactive against *Mabs*. Among the few clinically

235   used drugs for the treatment of *Mabs* infection, cefoxitin, amikacin, imipenem and

236   erythromycin exhibit moderate activity *in vitro* on agar plates with MICs ranging from 60-125

237   μM, whereas clarithromycin demonstrated the highest activity with an MIC value of 4 μM.

10

238   Because clarithromycin and imipenem exhibit different physicochemical properties (high

239   molecular weight and hydrophobicity for clarithromycin versus low molecular weight and

240   hydrophilicity for imipenem), they were further investigated for their *in vivo* therapeutic

241   efficacy in *Mabs*-infected ZF.

242

243   **In vivo susceptibility of *M. abscessus* to clarithromycin**

244   Due to insufficient information concerning the mechanisms of drug uptake by ZF

245   embryos/larvae, a wide range of concentrations, spanning from 6.6 μM-668 μM of

246   clarithromycin (corresponding to 1.7X to 170X the *in vitro* MIC value obtained using the

247   microdilution method) was tested. Supplementation of the embryo-containing water with low

248   or intermediate doses (1.7X and 17X the MIC, respectively) displayed no toxicity as measured

249   by larval survival, while used at the highest dose tested (170X MIC), a 10% reduction in larval

250   survival was observed at 9dpi, with respect to the control group in which water was

251   supplemented with 1% DMSO (26) (Figure 3A). Embryos that develop in the presence of high

252   doses of clarithromycin had a curved body trunk with uninflated swim bladder as compared to

253   the DMSO control embryos (Figure 3A, inset). These phenotypic alterations were hardly

254   observed when exposed to intermediate or low doses of clarithromycin (data not shown).

255   Nevertheless, since these developmental abnormalities essentially occurred at the highest

256   doses, we next assessed the *in vivo* efficacy of clarithromycin in *Mabs*-infected embryos. No

257   significant increased survival was found when infected-embryos were exposed to low and

258   intermediate drug concentrations (Figure 3B). In contrast, high doses extended the life span of

259   infected embryos and fully protected the infected embryos up to 9dpi, when the first embryo

260   started to dye, which coincidently, corresponded to the toxicity-induced-killing effect (Figure

261   3A). This shows that clarithromycin, using the highest regimen, is efficient in the ZF test system.

11

262   **Effects of clarithromycin on ZF survival, bacterial burden and abscesses**

263   Increased survival was associated with lower bacterial burdens after 3dpi in the presence

264   of the highest dose (170X MIC), as determined quantitatively by CFU plating (Figure 3C),

265   whereas treatment with the low or intermediate doses failed to restrict mycobacterial growth.

266   *In vivo* drug efficacy was next monitored by time-lapse fluorescence microscopy (Figure 3D).

267   Injection of *Mabs* led to the appearance of rapidly growing infection foci and abscesses in the

268   larval brain at 3dpi, as reported previously (19). Imaging the same infected embryos at 3 and

269   5dpi revealed that abscesses within the brain were already reduced at 3dpi when treated with

270   high drug concentrations and this effect in reducing the clinical signs of the infection was even

271   more accentuated at 5dpi. There was no visible reduction of the infection at 5dpi in ZF treated

272   with low or intermediate drug concentrations, consistent with the survival curves and kinetic of

273   bacterial growth. A quantitative analysis revealed that high doses of clarithromycin reduced by

274   50% the number of embryos with abscesses (Figure 3E), and this drug effect was apparent in

275   both the brain and the spinal cord (Figure 3F), albeit the impact of lower drug concentrations

276   was not significant. This indicates that clarithromycin exerts a beneficial effect by inhibiting

277   mycobacterial growth, preventing the development of abscesses within the CNS and protecting

278   the embryos from bacterial killing.

279

280   **Effects of imipenem on ZF survival and reduction of the pathological signs**

281   To further confirm and extend the impact and usefulness of this biological system with

282   respect to *in vivo* drug testing, embryos were exposed to water-soluble imipenem, a clinically

283   relevant drug against *Mabs* known to act on L,D-transpeptidases (17, 27). A wide range of

284   concentrations was tested, corresponding to 0.5X to 28X MIC of imipenem, and neither signs of

285   toxicity-induced-killing nor developmental abnormalities were detected even at the highest

286 dose (data not shown). When assessing the effect of imipenem on infected ZF, no increased

287 survival was found with low drug concentrations. However, treatment with intermediate doses

288 led to a significant increase in survival and 100% of protection was observed in the presence of

289 this highest drug concentration (Figure 4A). These survival rates correlated with the CFU loads

290 as intermediate and high doses of imipenem started to restrict bacterial growth at 3dpi (after

291 two days of drug treatment) (Figure 4B). With the highest dose, there was a 3 Log_{10} decline in

292 the CFU at 5dpi (four days of treatment) compared with the untreated control group. Time-

293 lapse fluorescence microscopy further confirmed the *in vivo* efficacy of imipenem, illustrating

294 the inhibition of bacterial growth and disappearance of abscesses in the larval brain at 3 and

295 5dpi, respectively (Figure 4C). There was no visible reduction of the infection at 5dpi when

296 treated with low imipenem doses, consistent with the survival curves and kinetic of bacterial

297 growth. High doses significantly reduced the proportion of embryos with abscesses (Figure 4D),

298 a phenotypic effect that was particularly apparent in the brain on infected embryos (Figure 4E),

299 indicating that imipenem reduces the pathology signs of the infection.

300   These results also prompted us to examine whether imipenem can counteract/alter the

301 progression of an already established infection, especially when given at 3dpi when brain

302 abscesses are already apparent (Figure S1A). Death curves indicate that treatment with high

303 doses of imipenem effectively extended the life span of embryos with pre-existing abscesses

304 (Figure S1B). A large proportion (more than 60%) of the treated embryos survived to the

305 infection compared to 10% for the non-treated individuals (P=0.008). The remaining 40%

306 embryos that died despite the treatment showed increased bacterial loads in the CNS (data not

307 shown). The increased index of protection rate was associated to a significant decrease in the

308 number of embryos with abscesses (Figure S1C), particularly within the brain (Figure S1D). This

309   "curative" protocol shows that imipenem was able to cure embryos with pre-existing abscesses

310   and to protect severely infected ZF.

311

312   ***In vivo* inhibition activity of imipenem on mycobacterial cording**

313   Rough *Mabs* displays a dry texture with organized serpentine cords on agar plates (19, 28,

314   29) and large bacterial clumps consisting mainly of cords in liquid cultures (19). Our recent

315   studies also unraveled the presence of serpentine cords within the brain or spinal cord of

316   embryos infected with the rough morphotype and emphasized the role of cording in immune

317   evasion by preventing phagocytosis of *Mabs* by macrophages and neutrophils (19). Since cords

318   are easy to visualize and to numerate by fluorescence microscopy (Figure 5A), and because they

319   promote extracellular replication, abscess formation and tissue damage, we investigated

320   whether exposure of infected embryos to imipenem may also affect the development of

321   mycobacterial cords. Figure 5B shows the presence of multiple cords within the brain at 5dpi

322   (left panel) and the impact of imipenem treatment on the number of cords (right panel).

323   Quantitative analysis of the percentage of embryos with cords at 4dpi is shown in Figure

324   5C. The presence of low doses of imipenem has little impact on mycobacterial cords, although a

325   reduction of the number of embryos with cords was detected at 4dpi. However, this effect was

326   more pronounced with higher drug concentrations with only 20% of cord-laden embryos at

327   4dpi (compared to 60% for untreated embryos at 4dpi). This dose-dependent effect occurred

328   essentially within the CNS whilst reduction of cord formation within the vasculature was not

329   significant (Figure 5D).

330

DISCUSSION

At a basic research level, the appropriate use of animal models can help to improve our understanding of host-pathogen interactions. At a more applied level, preclinical evaluation of new drug compounds requires *in vivo* testing prior these can advance along the development pipeline. However, *in vivo* animal studies, when possible, are usually costly and time-consuming and present a major bottleneck in drug developments. Implementation of novel approaches, expected to accelerate the *in vivo* efficacy assessment of drugs, is particularly justified in two cases. First, such systems are useful for bacterial infections requiring extended periods of drug treatment such as mice infected with *M. tuberculosis,* for which rapid *in vivo* assessment of drug efficacy directly in infected mice using fluorescence imaging (30) or using improved firefly luciferase (31) were elegantly demonstrated. We similarly show in this study how the use of fluorescence imaging can be useful in evaluating antimicrobial activity against *Mabs*. Second, alternative biological systems are particularly relevant for infections lacking of a permissive animal model. In this context, we recently demonstrated the high susceptibility of ZF embryos to *Mabs* and how the number of CNS abscesses may represent a marker for establishing *in vivo* antibiotic activity against *Mabs*.

Due to its intrinsic and acquired resistance to commonly used antibiotics, treatment becomes more complicated, thereby leading to high failure rates, stressing the need for new drug discovery. One of the key steps of drug discovery process is to identify and evaluate the *in vitro* and *in vivo* potential of new hits against *Mabs,* which pre-requires adequate animal models. Assessing the murine model which, following *i.v.* or aerosol infection, led only to transient colonization. Therefore, the natural course of infection in immune-competent BALB/c mice impedes its use as a valuable animal model for drug susceptibility testing. Comparatively, SCID mouse model has been shown to produce a chronic infection of *Mabs*, but this model has

15

355 not been used for drug testing (29, 32). However, granulocyte-macrophage colony-stimulating

356 (GM-CSF) knockout mice have recently been used to develop a new animal model of persistent

357 pulmonary *Mabs* infection that can be used for preclinical efficacy testing of anti-microbial

358 drugs (15). In particular, azithromycin treatment of *Mabs*-infected GM-CSF KO mice resulted in

359 a lower bacterial burden in the lungs and spleen, weight gain and significant improvement in

360 lung pathology (15). Another report proposed Nude mice as an adequate model for *in vivo*

361 chemotherapy studies (16). However, both models raised the question of the adaptive

362 response in addition to the antibiotic activity in eradicating the bacilli. It was previously shown

363 that, albeit being a rapid-growing mycobacterium, *Mabs* infection was only controlled in mice

364 with a functional adaptive immune response (22), as compared to *M. chelonae*, which was

365 cleared even in T cell-deficient mice. In addition, and despite the fact that both immune-

366 compromised mice present a significant advance as compared to wild-type mice in preclinical

367 assessments, these models remain costly and time-consuming and remain most likely not

368 suitable for a general use in drug screening campaigns.

369   New non-mammalian models of infection have been developed, including *Drosophila*

370 *melanogaster* (33, 34), *Caenorhabditis elegans* (35) or *Danio rerio* (36, 37) which offer several

371 advantages in terms of speed, cost, technical convenience and ethical acceptability over the

372 mouse model. However, very few of these alternative models, except for the recent Drosophila

373 model (34), have been reported for antibiotic assessments against *Mabs*. In this study, we

374 propose the ZF model, to visualize by non-invasive imaging the progressive infection of *Mabs* in

375 live animals, and to quantifying the effect of drug treatment. We successfully investigated the

376 suitability and sensitivity of two clinically relevant drugs, clarithromycin and imipenem, to

377 visualize in a dose- and time-dependent manner the dynamics of cord and abscess

378 formation/resorption. One major advantage of this model compared to mice is the ease and

379   rapidity of experimentation within a restricted time scale and low cost. That both drugs had a

380   positive impact in terms of embryo survival was correlated to a significant reduction in the

381   number of CFU and abscesses, demonstrating a proof of concept that ZF embryos are suitable

382   for drug efficacy testing. Since *in vitro* studies demonstrated decreased MICs in the presence of

383   imipenem for clarithromycin, minocycline, levofloxacin and moxifloxacin (38), future work

384   should also address the *in vivo* efficacy of these drug combinations using the *Mabs*/ZF couple.

385   It is, however, noteworhty that despite of their unique features for the *in vivo* drug testing,

386   ZF embryos also present several disadvantages over mammalian models. In particular, there are

387   some important anatomical differences between ZF embryos and mammmals such as gills

388   instead of lungs, hematopoiesis occurring in the anterioir kidney instead of the bone marrow,

389   lack on discernable lymph nodes as well as a very different reproductive system. In addition,

390   the natural lack of an adaptive immunity early in the development is very likely to affect the

391   outcome of the infection, thus making it difficult to directly correlating data obtained in ZF and

392   in humans. In addition, as shown in this study, embryos allow to describing effects of antibiotics

393   during acute *Mabs* infections but not during the chronic stages of the disease, which can be

394   better modelled for instance using immuno-compromized mice (15). In a similar vein, since

395   pharmacokinetics in are not known in ZF, it remains difficult at this stage to directly transpose

396   the MIC data obtained in ZF to humans. As a consequence, this biological system should

397   essentially be regarded as an early model for pre-clinical drug testing and/or to select for new

398   active compounds which should then be evaluated in other models before clinical trials.

399   Nevertheless, the perspectives of application of these findings are multiple. First, this

400   method could be implemented to address the *in vivo* drug susceptibility profiles of clinical

401   isolates that include strains from CF and non-CF patients, as *Mabs* clinical strains are not

402   uniformly susceptible to the currently used antibiotics. Due to these strain-to-strain variations

403   (17, 39), no optimal regimen has been established to cure *Mabs* infections and determining the

404   susceptibility/resistance profile of clinical strains may greatly help the clinician to select optimal

405   drug treatments. It is worth mentioning that for this particular application, no absolute

406   requirement for the tested strains to carry pTEC27 is needed, as visualization of fluorescent

407   bacteria is not necessary if assessing ZF survival only. Second, since the ZF is particularly

408   amenable to mimic a CF-like micro-environment, by silencing the *cftr* expression level (40), this

409   system would also allow to comparing the therapeutic efficacy of clarithromycin and imipenem

410   (and perhaps other antibiotics) in a *cftr*-deficient environment as it remains to be established

411   whether a defect in CFTR affects susceptibility to drugs. Third, this method could be further

412   exploited to compare the intrinsic activity of antibiotics *in vivo* in embryos infected with the

413   three species of the *M. abscessus* complex - *M. abscessus sensu stricto*, *M. massiliense*, and *M.*

414   *bolletii* - which are known to respond differently to antibiotics *in vitro* (41, 42).

415   Finally, the ZF embryo is particularly suited for high throughput screening as shown recently

416   for *M. marinum* (36, 43, 44). Work is currently in progress in our laboratory to develop an *in vivo*

417   platform for high-throughput screening of molecules against *Mabs* in order to speed up the

418   process of identifying promising drug candidates, particularly warranted due to the extreme

419   resistance of *Mabs* to most current antibiotics.

420

431

432

REFERENCES

1. **Medjahed, H., J. L. Gaillard, and J. M. Reyrat.** 2010. Mycobacterium abscessus: a new player in the mycobacterial field. Trends Microbiol **18:**117-23.

2. **Petrini, B.** 2006. Mycobacterium abscessus: an emerging rapid-growing potential pathogen. Apmis **114:**319-28.

3. **Roux, A. L., E. Catherinot, F. Ripoll, N. Soismier, E. Macheras, S. Ravilly, G. Bellis, M. A. Vibet, E. Le Roux, L. Lemonnier, C. Gutierrez, V. Vincent, B. Fauroux, M. Rottman, D. Guillemot, and J. L. Gaillard.** 2009. Multicenter study of prevalence of nontuberculous mycobacteria in patients with cystic fibrosis in france. J Clin Microbiol **47:**4124-8.

4. **Sanguinetti, M., F. Ardito, E. Fiscarelli, M. La Sorda, P. D'Argenio, G. Ricciotti, and G. Fadda.** 2001. Fatal pulmonary infection due to multidrug-resistant Mycobacterium abscessus in a patient with cystic fibrosis. J Clin Microbiol **39:**816-9.

5. **Gilljam, M., H. Schersten, M. Silverborn, B. Jonsson, and A. Ericsson Hollsing.** 2010. Lung transplantation in patients with cystic fibrosis and Mycobacterium abscessus infection. J Cyst Fibros **9:**272-6.

6. **Aitken, M. L., A. Limaye, P. Pottinger, E. Whimbey, C. H. Goss, M. R. Tonelli, G. A. Cangelosi, M. A. Dirac, K. N. Olivier, B. A. Brown-Elliott, S. McNulty, and R. J. Wallace, Jr.** 2012. Respiratory outbreak of Mycobacterium abscessus subspecies massiliense in a lung transplant and cystic fibrosis center. Am J Respir Crit Care Med **185:**231-2.

7. **Wallace, R. J., Jr., B. A. Brown, and D. E. Griffith.** 1998. Nosocomial outbreaks/pseudo-outbreaks caused by nontuberculous mycobacteria. Annu Rev Microbiol **52:**453-90.

8. **Viana-Niero, C., K. V. Lima, M. L. Lopes, M. C. Rabello, L. R. Marsola, V. C. Brilhante, A. M. Durham, and S. C. Leao.** 2008. Molecular characterization of Mycobacterium massiliense and Mycobacterium bolletii in isolates collected from outbreaks of infections after laparoscopic surgeries and cosmetic procedures. J Clin Microbiol **46:**850-5.

458   9.   **Zelazny, A. M., J. M. Root, Y. R. Shea, R. E. Colombo, I. C. Shamputa, F. Stock, S. Conlan, S.**

459   **McNulty, B. A. Brown-Elliott, R. J. Wallace, Jr., K. N. Olivier, S. M. Holland, and E. P. Sampaio.**

460   2009. Cohort study of molecular identification and typing of Mycobacterium abscessus,

461   Mycobacterium massiliense, and Mycobacterium bolletii. J Clin Microbiol **47:**1985-95.

462   10. **Cullen, A. R., C. L. Cannon, E. J. Mark, and A. A. Colin.** 2000. Mycobacterium abscessus infection

463   in cystic fibrosis. Colonization or infection? Am J Respir Crit Care Med **161:**641-5.

464   11. **Tomashefski, J. F., Jr., R. C. Stern, C. A. Demko, and C. F. Doershuk.** 1996. Nontuberculous

465   mycobacteria in cystic fibrosis. An autopsy study. Am J Respir Crit Care Med **154:**523-8.

466   12. **Rodriguez, G., M. Ortegon, D. Camargo, and L. C. Orozco.** 1997. Iatrogenic Mycobacterium

467   abscessus infection: histopathology of 71 patients. Br J Dermatol **137:**214-8.

468   13. **Griffith, D. E., T. Aksamit, B. A. Brown-Elliott, A. Catanzaro, C. Daley, F. Gordin, S. M. Holland,**

469   **R. Horsburgh, G. Huitt, M. F. Iademarco, M. Iseman, K. Olivier, S. Ruoss, C. F. von Reyn, R. J.**

470   **Wallace, Jr., and K. Winthrop.** 2007. An official ATS/IDSA statement: diagnosis, treatment, and

471   prevention of nontuberculous mycobacterial diseases. Am J Respir Crit Care Med **175:**367-416.

472   14. **Jeon, K., O. J. Kwon, N. Y. Lee, B. J. Kim, Y. H. Kook, S. H. Lee, Y. K. Park, C. K. Kim, and W. J.**

473   **Koh.** 2009. Antibiotic treatment of Mycobacterium abscessus lung disease: a retrospective

474   analysis of 65 patients. Am J Respir Crit Care Med **180:**896-902.

475   15. **De Groote, M. A., L. Johnson, B. Podell, E. Brooks, R. Basaraba, and M. Gonzalez-Juarrero.**

476   2013. GM-CSF knockout mice for preclinical testing of agents with antimicrobial activity against

477   Mycobacterium abscessus. J Antimicrob Chemother **In Press.**

478   16. **Lerat, I., E. Cambau, R. Roth Dit Bettoni, J. L. Gaillard, V. Jarlier, C. Truffot, and N. Veziris.** 2013.

479   In vivo evaluation of antibiotic activity against Mycobacterium abscessus. J Infect Dis **In Press.**

480   17. **Lavollay, M., V. Dubee, B. Heym, J. L. Herrmann, J. L. Gaillard, L. Gutmann, M. Arthur, and J. L.**

481   **Mainardi.** 2013. In vitro activity of cefoxitin and imipenem against Mycobacterium abscessus

482   complex. Clin Microbiol Infect **In Press.**

483   18.   **Cortes, M., A. K. Singh, J. M. Reyrat, J. L. Gaillard, X. Nassif, and J. L. Herrmann.** 2011.

484   Conditional gene expression in Mycobacterium abscessus. PLoS One **6:**e29306.

485   19.   **Bernut, A., J. L. Herrmann, K. Kissa, J. F. Dubremetz, J. L. Gaillard, G. Lutfalla, and L. Kremer.**

486   The zebrafish model reveals specific pathophysiological traits and neurotropism of

487   Mycobacterium abscessus. **Under revision**.

488   20.   **Talati, N. J., N. Rouphael, K. Kuppalli, and C. Franco-Paredes.** 2008. Spectrum of CNS disease

489   caused by rapidly growing mycobacteria. Lancet Infect Dis **8:**390-8.

490   21.   **Lee, M. R., A. Cheng, Y. C. Lee, C. Y. Yang, C. C. Lai, Y. T. Huang, C. C. Ho, H. C. Wang, C. J. Yu,**

491   **and P. R. Hsueh.** 2011. CNS infections caused by Mycobacterium abscessus complex: clinical

492   features and antimicrobial susceptibilities of isolates. J Antimicrob Chemother **67:**222-5.

493   22.   **Rottman, M., E. Catherinot, P. Hochedez, J. F. Emile, J. L. Casanova, J. L. Gaillard, and C.**

494   **Soudais.** 2007. Importance of T cells, gamma interferon, and tumor necrosis factor in immune

495   control of the rapid grower Mycobacterium abscessus in C57BL/6 mice. Infect Immun **75:**5898-

496   907.

497   23.   **Catherinot, E., J. Clarissou, G. Etienne, F. Ripoll, J. F. Emile, M. Daffe, C. Perronne, C. Soudais, J.**

498   **L. Gaillard, and M. Rottman.** 2007. Hypervirulence of a rough variant of the Mycobacterium

499   abscessus type strain. Infect Immun **75:**1055-8.

500   24.   **Woods, G. L., B. A. Brown-Elliott, P. S. Conville, E. P. Desmond, G. S. Hall, G. Lin, G. E. Pfyffer, J.**

501   **C. Ridderhof, S. H. Siddiqi, R. J. Wallace, N. G. Warren, and F. G. Witebsky.** 2011. Susceptibility

502   testing of mycobacteria, nocardiae, and other aerobic actinomycetes; approved standard,

503   Second Edition. M24-A2. Clinical and Laboratory Standards Institute, Wayne, PA.

504   25.   **Lamason, R. L., M. A. Mohideen, J. R. Mest, A. C. Wong, H. L. Norton, M. C. Aros, M. J. Jurynec,**

505   **X. Mao, V. R. Humphreville, J. E. Humbert, S. Sinha, J. L. Moore, P. Jagadeeswaran, W. Zhao, G.**

506   **Ning, I. Makalowska, P. M. McKeigue, D. O'Donnell, R. Kittles, E. J. Parra, N. J. Mangini, D. J.**

507   **Grunwald, M. D. Shriver, V. A. Canfield, and K. C. Cheng.** 2005. SLC24A5, a putative cation

508   exchanger, affects pigmentation in zebrafish and humans. Science **310:**1782-6.

509   26.   **Adams, K. N., K. Takaki, L. E. Connolly, H. Wiedenhoft, K. Winglee, O. Humbert, P. H. Edelstein,**

510   **C. L. Cosma, and L. Ramakrishnan.** 2011. Drug tolerance in replicating mycobacteria mediated

511   by a macrophage-induced efflux mechanism. Cell **145:**39-53.

512   27.   **Lavollay, M., M. Fourgeaud, J. L. Herrmann, L. Dubost, A. Marie, L. Gutmann, M. Arthur, and J.**

513   **L. Mainardi.** 2011. The peptidoglycan of Mycobacterium abscessus is predominantly cross-

514   linked by L,D-transpeptidases. J Bacteriol **193:**778-82.

515   28.   **Medjahed, H., and J. M. Reyrat.** 2009. Construction of Mycobacterium abscessus defined

516   glycopeptidolipid mutants: comparison of genetic tools. Appl Environ Microbiol **75:**1331-8.

517   29.   **Howard, S. T., E. Rhoades, J. Recht, X. Pang, A. Alsup, R. Kolter, C. R. Lyons, and T. F. Byrd.**

518   2006. Spontaneous reversion of Mycobacterium abscessus from a smooth to a rough

519   morphotype is associated with reduced expression of glycopeptidolipid and reacquisition of an

520   invasive phenotype. Microbiology **152:**1581-90.

521   30.   **Zelmer, A., P. Carroll, N. Andreu, K. Hagens, J. Mahlo, N. Redinger, B. D. Robertson, S. Wiles, T.**

522   **H. Ward, T. Parish, J. Ripoll, G. J. Bancroft, and U. E. Schaible.** 2012. A new in vivo model to test

523   anti-tuberculosis drugs using fluorescence imaging. J Antimicrob Chemother **67:**1948-60.

524   31.   **Andreu, N., A. Zelmer, S. L. Sampson, M. Ikeh, G. J. Bancroft, U. E. Schaible, S. Wiles, and B. D.**

525   **Robertson.** 2013. Rapid in vivo assessment of drug efficacy against Mycobacterium tuberculosis

526   using an improved firefly luciferase. J Antimicrob Chemother.

527   32.   **Byrd, T. F., and C. R. Lyons.** 1999. Preliminary characterization of a Mycobacterium abscessus

528   mutant in human and murine models of infection. Infect Immun **67:**4700-7.

529   33.   **Oh, C. T., C. Moon, M. S. Jeong, S. H. Kwon, and J. Jang.** 2013. Drosophila melanogaster model

530   for Mycobacterium abscessus infection. Microbes Infect.

531   34.   **Oh, C. T., C. Moon, O. K. Park, S. H. Kwon, and J. Jang.** 2014. Novel drug combination for

532   Mycobacterium abscessus disease therapy identified in a Drosophila infection model. J

533   Antimicrob Chemother.

23

534   35.   **Squiban, B., and C. L. Kurz.** 2011. C. elegans: an all in one model for antimicrobial drug

535   discovery. Curr Drug Targets **12:**967-77.

536   36.   **Takaki, K., C. L. Cosma, M. A. Troll, and L. Ramakrishnan.** 2012. An in vivo platform for rapid

537   high-throughput antitubercular drug discovery. Cell Rep **2:**175-84.

538   37.   **Takaki, K., J. M. Davis, K. Winglee, and L. Ramakrishnan.** 2013. Evaluation of the pathogenesis

539   and treatment of Mycobacterium marinum infection in zebrafish. Nat Protoc **8:**1114-24.

540   38.   **Miyasaka, T., H. Kunishima, M. Komatsu, K. Tamai, K. Mitsutake, K. Kanemitsu, Y. Ohisa, H.**

541   **Yanagisawa, and M. Kaku.** 2007. In vitro efficacy of imipenem in combination with six

542   antimicrobial agents against Mycobacterium abscessus. Int J Antimicrob Agents **30:**255-8.

543   39.   **Shen, G. H., B. D. Wu, S. T. Hu, C. F. Lin, K. M. Wu, and J. H. Chen.** 2010. High efficacy of

544   clofazimine and its synergistic effect with amikacin against rapidly growing mycobacteria. Int J

545   Antimicrob Agents **35:**400-4.

546   40.   **Phennicie, R. T., M. J. Sullivan, J. T. Singer, J. A. Yoder, and C. H. Kim.** 2010. Specific resistance

547   to Pseudomonas aeruginosa infection in zebrafish is mediated by the cystic fibrosis

548   transmembrane conductance regulator. Infect Immun **78:**4542-50.

549   41.   **Bastian, S., N. Veziris, A. L. Roux, F. Brossier, J. L. Gaillard, V. Jarlier, and E. Cambau.** 2011.

550   Assessment of clarithromycin susceptibility in strains belonging to the Mycobacterium abscessus

551   group by erm(41) and rrl sequencing. Antimicrob Agents Chemother **55:**775-81.

552   42.   **Kim, H. Y., B. J. Kim, Y. Kook, Y. J. Yun, J. H. Shin, B. J. Kim, and Y. H. Kook.** 2010.

553   Mycobacterium massiliense is differentiated from Mycobacterium abscessus and

554   Mycobacterium bolletii by erythromycin ribosome methyltransferase gene (erm) and

555   clarithromycin susceptibility patterns. Microbiol Immunol **54:**347-53.

556   43.   **Carvalho, R., J. de Sonneville, O. W. Stockhammer, N. D. Savage, W. J. Veneman, T. H.**

557   **Ottenhoff, R. P. Dirks, A. H. Meijer, and H. P. Spaink.** 2011. A high-throughput screen for

558   tuberculosis progression. PLoS One **6:**e16779.

559   44.   **Spaink, H. P., C. Cui, M. I. Wiweger, H. J. Jansen, W. J. Veneman, R. Marin-Juez, J. de**

560   **Sonneville, A. Ordas, V. Torraca, W. van der Ent, W. P. Leenders, A. H. Meijer, B. E. Snaar-**

561   **Jagalska, and R. P. Dirks.** 2013. Robotic injection of zebrafish embryos for high-throughput

562   screening in disease models. Methods **62:**246-54.

563

564

565   **FIGURE LEGENDS**

566

567   **Figure 1. Kinetics of colonization of *M. abscessus* in aerosolised or intravenously infected**

568   **BALB/c mice. (A)** Mice were aerosolized by 4 × 10^7 CFU/ml of *Mabs*. Animal were then

569   sacrificed at days 1, 3, 8, 27 prior to CFU counting in the liver, spleen and lungs. Results are

570   expressed as the log units of CFU. **(B)** Mice were challenged *i.v.* 10^6 CFU of *Mabs.* Animals were

571   then sacrificed at days 1, 15 and 30 to determine the CFU counts in the different organs.

572   Results are representative of 2-3 independent experiments and Log CFU are expressed as the

573   mean ± standard error (n=5-7 mice for each time point).

574

575   **Figure 2. Experimental protocol to assess the *in vivo* drug activity on *M. abscessus* infection.**

576   ZF embryos were *i.v.* infected with ≈300 CFU of *Mabs* expressing dtTomato and distributed and

577   incubated into 96-wells plate (1). From 1dpi, embryos were exposed to the drugs of interest

578   which were directly added to the wells. Drugs are then removed and daily renewed for 5 days

579   (2). To determinate the *in vivo* antibacterial effects of the drugs, the embryo survival, the

580   bacterial loads and the evolution of the infection process were monitored at a spatiotemporal

581   level by videomicroscopy (3).

582

583   **Figure 3. *In vivo* characterization of clarithromycin activity on *M. abscessus* infection. (A-F)**

584   Embryos were soaked in clarithromycin at 1.7X, MIC 17X or 170X the MIC for 5 days. The red

585   bar indicates the start and duration of treatment. **(A)** Survival of uninfected embryos treated

586   with various doses of clarithromycin and compared to mock controls (DMSO 1%) (n=20 for

587   each, representative of three independent experiments). Representative microscopy image of

588   an untreated (inset, upper panel) or drug treated-embryo (inset, lower panel) at 8dpf.

589   Clarithromycin appears toxic at the highest concentration as evidenced by the presence

590   development abnormalities and the increased mortality rate in the drug-exposed embryos

591   compared to the mock control (p=0.028, log-rank test). **(B)** Survival of infected *Mabs* treated at

592   various doses of clarithromycin and compared to untreated infected embryos (≈300 CFU, n=20,

593   representative of three independent experiments). A significant increased survival was

594   observed in the infected-embryos exposed to the highest drug concentration (p=0.029, log-rank

595   test). **(C)** Bacterial loads of untreated or treated-embryos (≈400 CFU). Results are expressed as

596   mean Log_{10} CFU per embryo from three independent experiments. A significant reduction in

597   bacterial burdens with 170X the MIC in drug treated-embryos is observed at 5dpi. **(D)**

598   Spatiotemporal visualization of the infection by *Mabs* expressing dtTomato (≈300 CFU) in

599   untreated or drug treated-embryos. The representative fluorescence and transmission overlay

600   of whole embryos are shown. The yolk is auto-fluorescent. **(E)** Frequency of abscesses in whole

601   untreated or drug treated-embryos over 13dpi (≈300 CFU; average of three independent

602   experiments). Infected embryos developed significantly less abscesses in the presence

603   clarithromycin at 170X the MIC than untreated infected-embryos. **(F)** Average localization of

604   abscesses of the infected embryos in (E). *Mabs*-infected ZF developed significantly less

605   abscesses within the brain and the spinal when exposed to the highest clarithromycin dose as

606   compared to untreated infected-ZF. For (c) statistics were calculated using one-way ANOVA or

607   for (e) and (f) with Fisher's exact test comparing each category of drug-treated embryos to

608   untreated control. Error bars represent the standard errors. **p<0.01.

609

610   **Figure 4. Imipenem treatment cures *M. abscessus*-infected embryos. (A-E)** From 1dpi,

611   embryos were exposed for 5 days to imipenem concentrations corresponding to 0.5X, 5X or 28X

612   the MIC. **(A)** Survival of infected *Mabs* R treated at various doses of imipenem and compared to

613   untreated infected embryos (≈300 CFU, n=20, representative of three independent

experiments). Survival of treated R-infected embryos is dose-dependent. Significant increased

survival was observed in infected-embryos exposed to 5 X and 28X MIC of imipenem. The red

bar indicates the start and duration of treatment. **(B)** Bacterial loads of untreated or imipenem

treated-embryos (≈400 CFU). Results are expressed as mean Log_{10} CFU per embryo from three

independent experiments. A significant decreased of bacterial loads is already observed after

3dpi in the 28X MIC imipenem treated-embryos. **(C)** Spatiotemporal visualization of the

infection by *Mabs* expressing dtTomato (≈300 CFU) in untreated or imipenem treated-embryos.

The representative fluorescence and transmission overlay of whole embryos are shown. **(D)**

Frequency of abscesses in whole untreated or imipenem-treated embryos over 13dpi (≈300

CFU, average of three independent experiments). Only the 28X MIC imipenem treated-embryos

developed significantly fewer abscesses than untreated infected-embryos. **(E)** Average

localization of abscesses of the infected embryos in (D). 5X and 28X MIC of imipenem treated-

embryos infected by *Mabs* developed fewer abscesses within the brain than untreated

infected-embryos. For (B) statistics were calculated using one-way ANOVA or for (D) and (E)

with Fisher's exact test comparing each category of imipenem-treated embryos to untreated

control. Error bars represent the standard error. *$p=0.02$, **$p<0.01$, ***$p<0.001$.

Figure 5. Imipenem treatment decreases the early pathophysiological signs within the CNS.

(A-D). dtTomato-expressing *Mabs* (≈300 CFU) are injected in 30hpf embryos (n=15, average of

three independent experiments). From 1dpi, embryos were exposed to imipenem at 0.5X, 5X or

28X MIC during 5 days. **(A)** Fluorescence microscopy of a typical R serpentine cord. Scale bar,

100μm. **(B)** Fluorescence and DIC overlay of whole heads of a 28X MIC imipenem-treated and

untreated infected embryos with red fluorescent *M. abs* showing serpentine cord (white

arrow). Scale bars, 100μm. **(C)** Percentage of embryos with cords in whole untreated and

638   imipenem-treated embryos at 4dpi. A significant reduction in the proportion of embryos with

639   cords was observed when embryos were treated with the highest (28X MIC) imipenem

640   concentration. **(D)** Average localization of cord of the infected embryos in (C). Infected embryos

641   treated with the intermediate (5X MIC) and high (28X MIC) imipenem doses developed

642   significantly fewer serpentine cords within the CNS compared to untreated infected-embryos.

643   For (C) and (D), statistics were calculated using Fisher's exact test comparing each category of

644   imipenem-treated embryos to untreated control. All results are expressed as the average from

645   three independent experiments and error bars represent the standard errors.
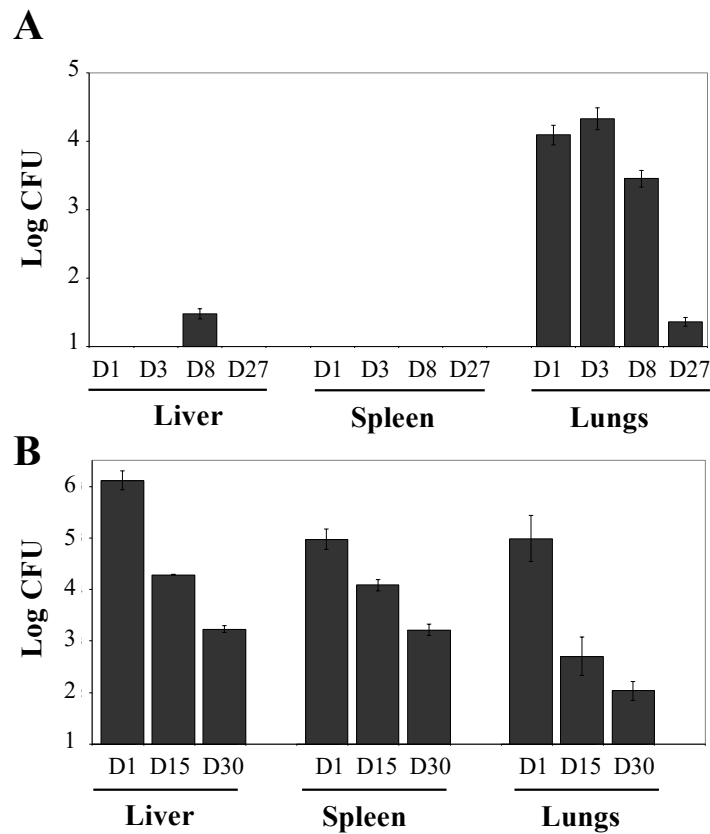
Figure 1. Kinetics of colonization of *M. abscessus* in aerosolised or intravenously infected BALB/c mice. **(A)** Mice were aerosolized by 4 × 10^7 CFU/ml of *Mabs*. Animal were then sacrificed at days 1, 3, 8, 27 prior to CFU counting in the liver, spleen and lungs. Results are expressed as the log units of CFU. **(B)** Mice were challenged *i.v.* 10^6 CFU of *Mabs.* Animals were then sacrificed at days 1, 15 and 30 to determine the CFU counts in the different organs. Results are representative of 2-3 independent experiments and Log CFU are expressed as the mean ± standard error (n=5-7 mice for each time point).
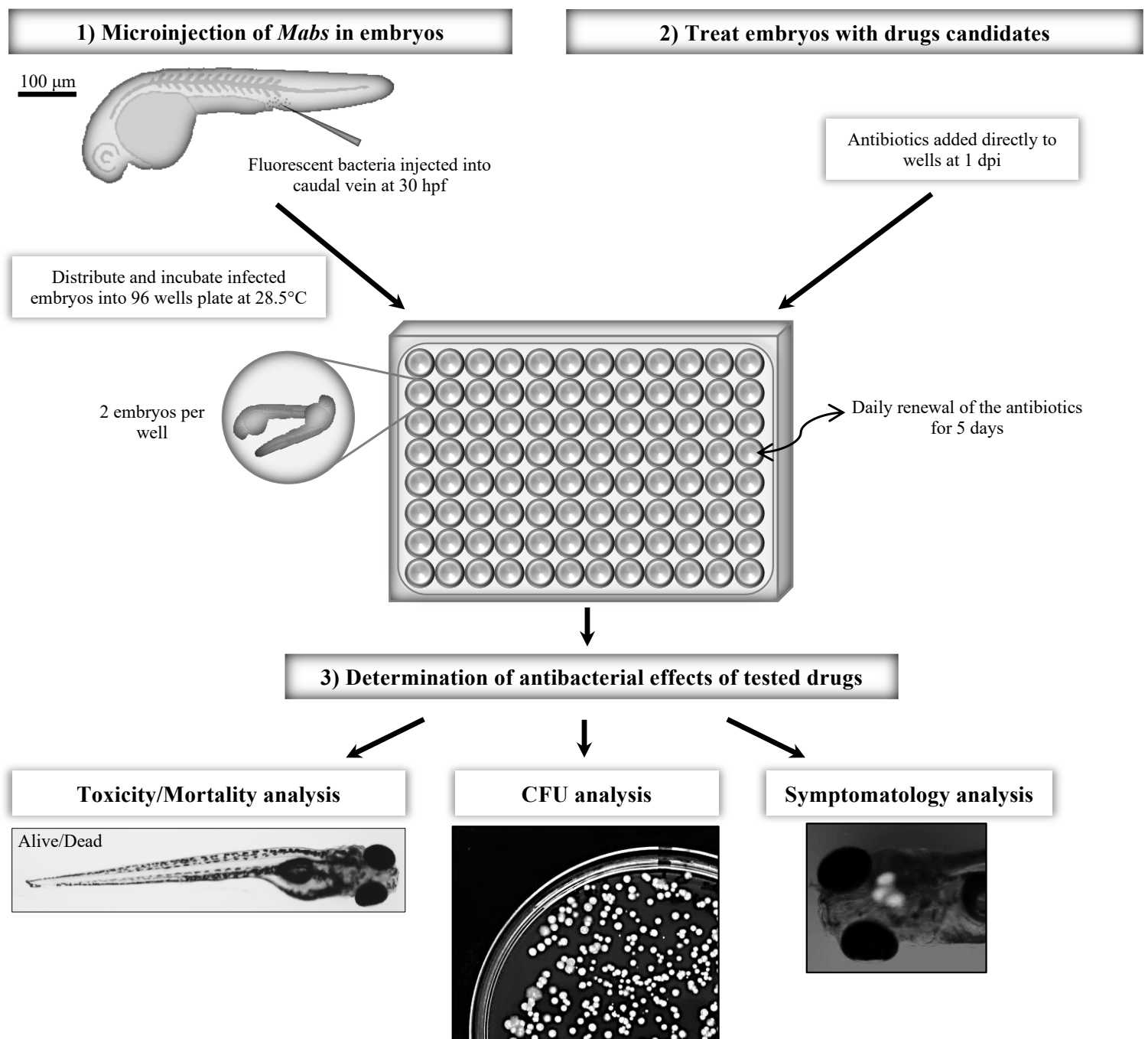
1) Microinjection of *Mabs* in embryos

100 μm

Fluorescent bacteria injected into
caudal vein at 30 hpf

Distribute and incubate infected
embryos into 96 wells plate at 28.5°C

2 embryos per
well

2) Treat embryos with drugs candidates

Antibiotics added directly to
wells at 1 dpi

Daily renewal of the antibiotics
for 5 days

3) Determination of antibacterial effects of tested drugs

Toxicity/Mortality analysis

Alive/Dead

CFU analysis

Symptomatology analysis

Figure 2. Experimental protocol to assess the *in vivo* drug activity on *M. abscessus* infection. ZF embryos were *i.v.* infected with ≈300 CFU of *Mabs* expressing dtTomato and distributed and incubated into 96-wells plate (1). From 1dpi, embryos were exposed to the drugs of interest which were directly added to the wells. Drugs are then removed and daily renewed for 5 days (2). To determinate the *in vivo* antibacterial effects of the drugs, the embryo survival, the bacterial loads and the evolution of the infection process were monitored at a spatiotemporal level by videomicroscopy (3).
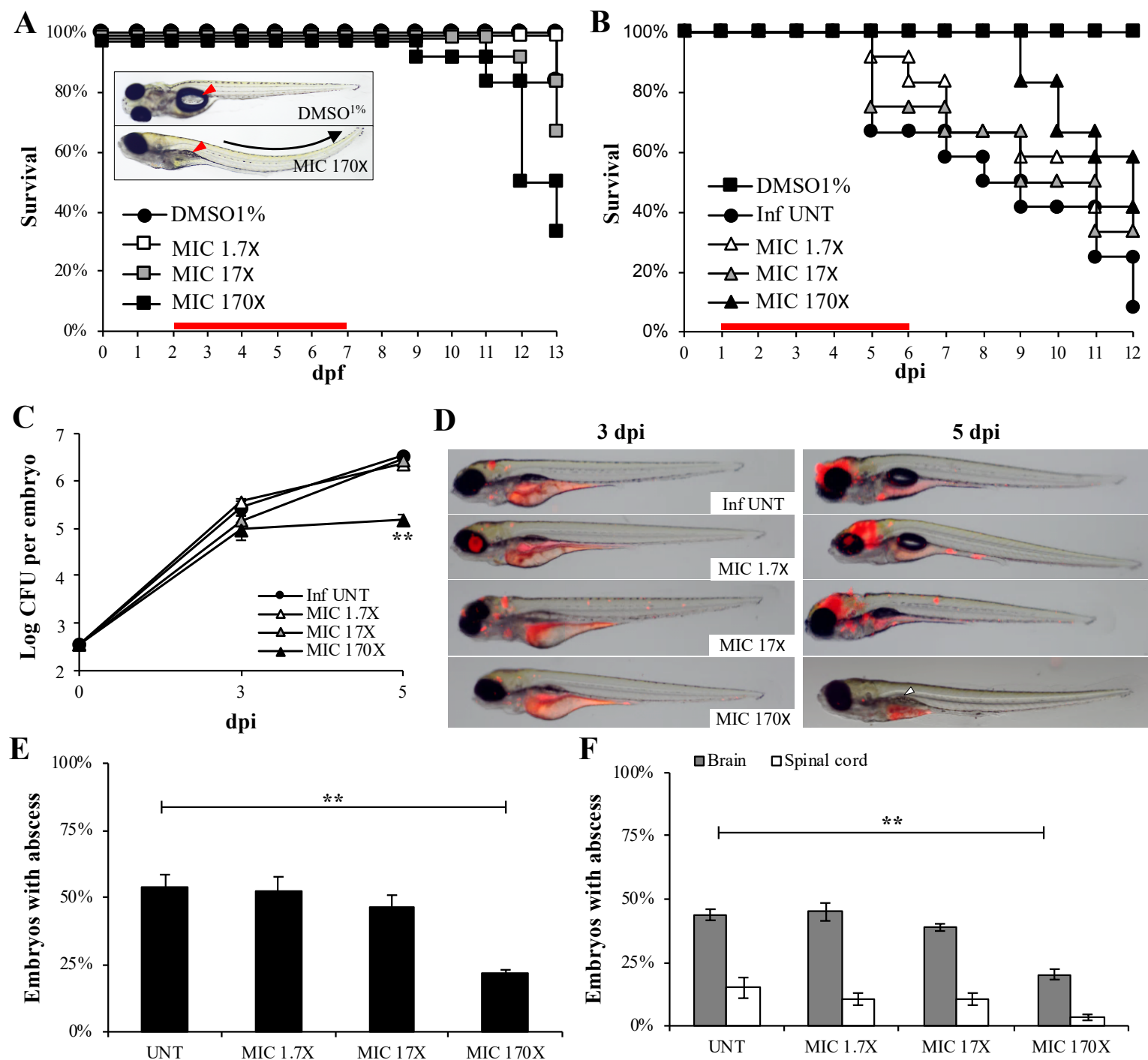
Figure 3. *In vivo* **characterization of clarithromycin activity on** *M. abscessus* **infection. (A-F)** Embryos were soaked in clarithromycin at 1.7X, MIC 17X or 170X the MIC for 5 days. The red bar indicates the start and duration of treatment. **(A)** Survival of uninfected embryos treated with various doses of clarithromycin and compared to mock controls (DMSO 1%) (n=20 for each, representative of three independent experiments). Representative microscopy image of an untreated (inset, upper panel) or drug treated-embryo (inset, lower panel) at 8dpf. Clarithromycin appears toxic at the highest concentration as evidenced by the presence development abnormalities and the increased mortality rate in the drug-exposed embryos compared to the mock control (p=0.028, log-rank test). **(B)** Survival of infected *Mabs* treated at various doses of clarithromycin and compared to untreated infected embryos (≈300 CFU, n=20, representative of three independent experiments). A significant increased survival was observed in the infected-embryos exposed to the highest drug concentration (p=0.029, log-rank test). **(C)** Bacterial loads of untreated or treated-embryos (≈400 CFU). Results are expressed as mean Log_{10} CFU per embryo from three independent experiments. A significant reduction in bacterial burdens with 170X the MIC in drug treated-embryos is observed at 5dpi. **(D)** Spatiotemporal visualization of the infection by *Mabs* expressing dtTomato (≈300 CFU) in untreated or drug treated-embryos. The representative fluorescence and transmission overlay of whole embryos are shown. The yolk is auto-fluorescent. **(E)** Frequency of abscesses in whole untreated or drug treated-embryos over 13dpi (≈300 CFU; average of three independent experiments). Infected embryos developed significantly less abscesses in the presence clarithromycin at 170X the MIC than untreated infected-embryos. **(F)** Average localization of abscesses of the infected embryos in (E). *Mabs*-infected ZF developed significantly less abscesses within the brain and the spinal when exposed to the highest clarithromycin dose as compared to untreated infected-ZF. For (c) statistics were calculated using one-way ANOVA or for (e) and (f) with Fisher's exact test comparing each category of drug-treated embryos to untreated control. Error bars represent the standard errors. **p<0.01.
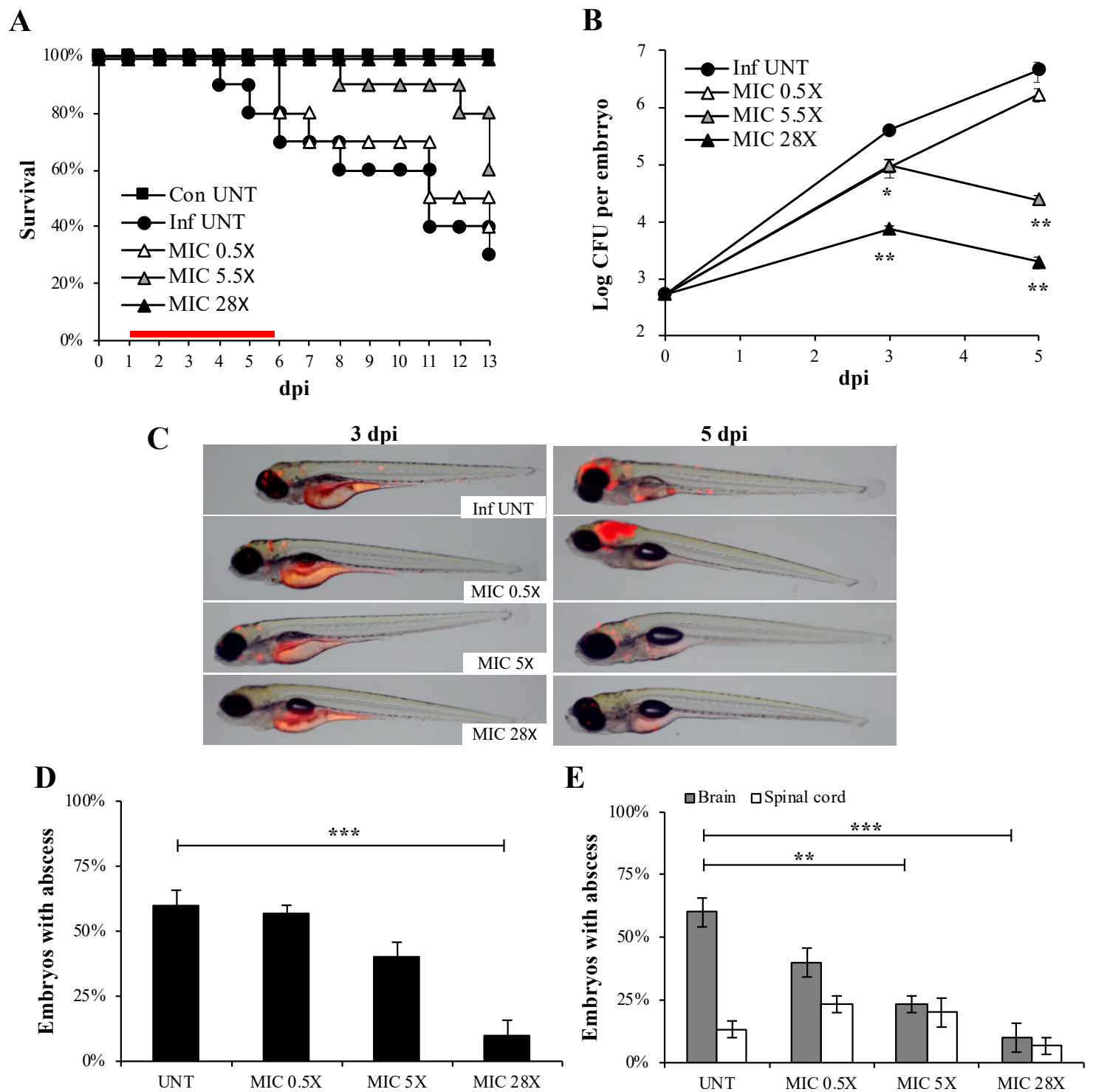
Figure 4. Imipenem treatment cures *M. abscessus*-infected embryos. (A-E) From 1dpi, embryos were exposed for 5 days to imipenem concentrations corresponding to 0.5X, 5X or 28X the MIC. **(A)** Survival of infected *Mabs* R treated at various doses of imipenem and compared to untreated infected embryos (≈300 CFU, n=20, representative of three independent experiments). Survival of treated R-infected embryos is dose-dependent. Significant increased survival was observed in infected-embryos exposed to 5 X and 28X MIC of imipenem. The red bar indicates the start and duration of treatment. **(B)** Bacterial loads of untreated or imipenem treated-embryos (≈400 CFU). Results are expressed as mean Log_{10} CFU per embryo from three independent experiments. A significant decreased of bacterial loads is already observed after 3dpi in the 28X MIC imipenem treated-embryos. **(C)** Spatiotemporal visualization of the infection by *Mabs* expressing dtTomato (≈300 CFU) in untreated or imipenem treated-embryos. The representative fluorescence and transmission overlay of whole embryos are shown. **(D)** Frequency of abscesses in whole untreated or imipenem-treated embryos over 13dpi (≈300 CFU, average of three independent experiments). Only the 28X MIC imipenem treated-embryos developed significantly fewer abscesses than untreated infected-embryos. **(E)** Average localization of abscesses of the infected embryos in (D). 5X and 28X MIC of imipenem treated-embryos infected by *Mabs* developed fewer abscesses within the brain than untreated infected-embryos. For (B) statistics were calculated using one-way ANOVA or for (D) and (E) with Fisher's exact test comparing each category of imipenem-treated embryos to untreated control. Error bars represent the standard error. *p=0.02, **p<0.01, ***p<0.001.

Figure 5. Imipenem treatment decreases the early pathophysiological signs within the CNS. (A-D). dtTomato-expressing *Mabs* (≈300 CFU) are injected in 30hpf embryos (n=15, average of three independent experiments). From 1dpi, embryos were exposed to imipenem at 0.5X, 5X or 28X MIC during 5 days. **(A)** Fluorescence microscopy of a typical R serpentine cord. Scale bar, 100µm. **(B)** Fluorescence and DIC overlay of whole heads of a 28X MIC imipenem-treated and untreated infected embryos with red fluorescent *M. abs* showing serpentine cord (white arrow). Scale bars, 100µm. **(C)** Percentage of embryos with cords in whole untreated and imipenem-treated embryos at 4dpi. A significant reduction in the proportion of embryos with cords was observed when embryos were treated with the highest (28X MIC) imipenem concentration. **(D)** Average localization of cord of the infected embryos in (C). Infected embryos treated with the intermediate (5X MIC) and high (28X MIC) imipenem doses developed significantly fewer serpentine cords within the CNS compared to untreated infected-embryos. For (C) and (D), statistics were calculated using Fisher's exact test comparing each category of imipenem-treated embryos to untreated control. All results are expressed as the average from three independent experiments and error bars represent the standard errors.

In vivo assessment of drug efficacy against *Mycobacterium abscessus* using the embryonic zebrafish test system

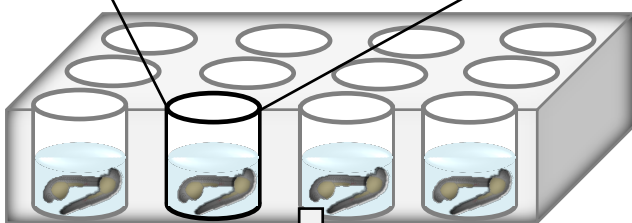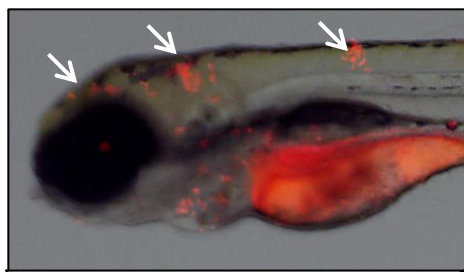Audrey Bernut[1], Vincent Le Moigne[3], Tiffany Lesne[1], Georges Lutfalla[1], Jean-Louis Herrmann[3] and Laurent Kremer[1,2,#]
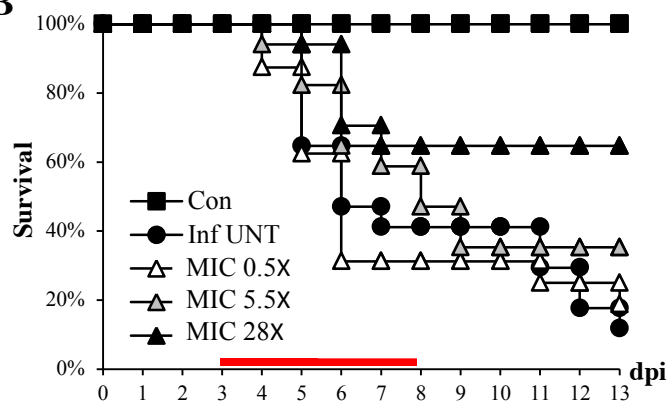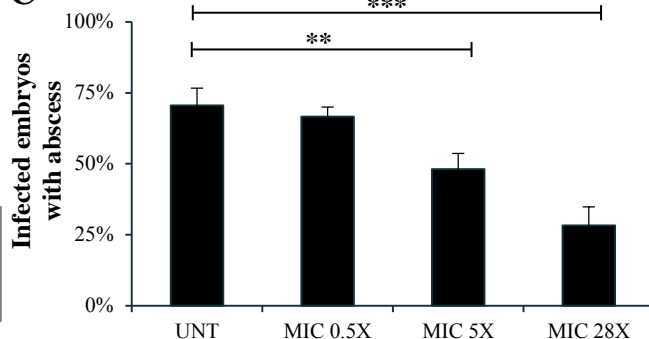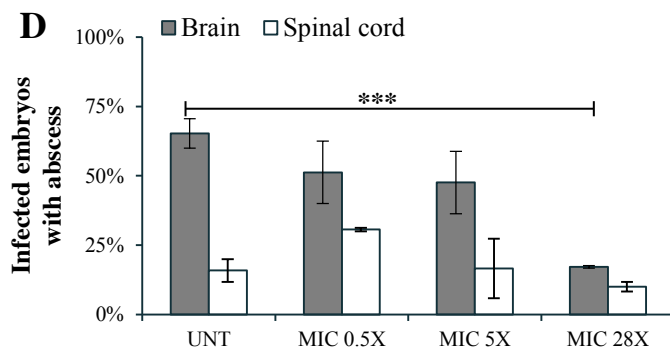
Figure S1. Exposure to imipenem overcomes and protects against severe *M. abscessus* infections. (A-C) dtTomato expressing *Mabs* (≈300 CFU) were injected in 30hpf embryos. From 3dpi, embryos were exposed during 5 days to imipenem at 0.5X, 5X or 28X MIC. **(A)** Schematic representation illustrating the "curing" protocol used as well as the infection status of the embryos at 3dpi (numerous abscesses within the CNS) when the drug treatment is applied. **(B)** Survival of infected *Mabs* treated at various doses of imipenem and compared to untreated infected embryos (n=20-30), representative of three independent experiments). A significant increased survival was observed in embryos exposed to the highest (28X MIC) imipenem dose. The red bar indicates the start and duration of treatment. **(C)** Frequency of *Mabs* abscesses in whole untreated or imipenem-treated embryos over 13dpi. Data are expressed as the average of three independent experiments. MIC 5X and MIC 28X imipenem treated-embryos infected by *Mabs* developed significantly fewer abscesses than untreated infected-embryos. **(D)** Average localization of abscesses of the infected embryos in (C). 28X MIC imipenem treated-embryos infected by *Mabs* developed significantly fewer abscesses within the brain than untreated infected-embryos. For (C) and (D) statistics were calculated using Fisher's exact test comparing each category of imipenem-treated embryos to untreated control. All results are expressed as the average from two or three independent experiments and error bars represent the standard errors. **p<0.01, ***p<0.001.

Table S1. Minimal inhibitory concentrations of several drugs against *M. abscessus* using the midrodilution method in cation-adjusted Mueller-Hinton (MH) broth or on LB agar. Antibiotics used in infected ZF are shown in bold. Results are expressed in µM and µg/ml.

Antibiotic	Molecular weight	Solvent	MIC MH broth		MIC LB agar	
			µM	µg/mL	µM	µg/mL
Clarithromycin	**748**	**DMSO**	**4**	**3.0**	**0.7**	**0.5**
Cefoxitin	427	DMSO	60	25.6	35	15
Amikacin	586	H_2O	125	73.25	26	15
Isoniazid	137	H_2O	1000	137	365	50
Erythromycin	734	DMSO	125	91.75	10	7.5
Imipenem	**299**	**H_2O**	**60**	**17.94**	**3.3**	**1**
Thiacetazone	236	DMSO	1000	236	42	10